Supplementary Information

Bimetallic nickel molybdenum nitride catalyst with low pressure and reduced hydrogen consumption for hydrogenation of dimethyl oxalate to ethanol: The impact of reduction temperature on catalytic performance.

Jiang Gong[a], Hanqing Zhang[a], Weihan Shu[a], Fengling Zheng[a], Hao Wang[a], Ni Zhang[a], Chuancai Zhang[a,] *, and Bin Dai[a,] *

[a] School of Chemistry and Chemical Engineering / State Key Laboratory Incubation Base for Green Processing of Chemical Engineering, Shihezi University, Shihezi 832003 (P.R. China)

*Corresponding author: E-mail addresses: zhangchuanc111@126.com (Chuancai Zhang)；
db_tea@shzu.edu.cn (Bin Dai)

1 Experimental Section

1.1 Chemicals

DMO ($C_4H_6O_4$, AR), nickel oxalate dihydrate ($NiC_2O_4{\cdot}2H_2O$, 99%), Nickel nitrate hexahydrate ($Ni(NO_3)_3{\cdot}6H_2O$, 99%), Molybdenum trioxide (MoO_3, 99.9%), ammonium molybdate tetrahydrate ($(NH_4)_6Mo_7O_{24}{\cdot}4H_2O$, 99%), ethylenediamine monohydrate ($C_2H_8N_2{\cdot}H_2O$, 98%), EtOH (C_2H_5OH, >99.5%), MG ($C_3H_6O_3$, >99%), EG ($(CH_2OH)_2$, >99%), and methyl acetate (MA; $C_3H_6O_2$, >99%) were used for the experiments.

1.2 Catalyst synthesis

1.2.1 Preparation of the Ni3Mo3N catalyst

The Ni_3Mo_3N catalyst was prepared using a method reported by Du et al[1] with some modifications. Specifically, first, 14.82 g of ammonium molybdate tetrahydrate and 2.22 g of nickel oxalate dihydrate were weighed and dissolved in 36 g of deionized water. After stirring this solution for 10 min, 26.58 g of ethylenediamine monohydrate was added and the mixture was stirred for another 10 min. Second, the mixed solution was transferred to an autoclave and heated at 130℃ for 8 h. After cooling the autoclave to room temperature, the resulting cake was filtered. Third, the filtered cake was washed with EtOH (Note: the obtained filtered cake is highly soluble in deionized water and cannot be washed using deionized water) and dried overnight at 100℃. Finally, the dried solid product underwent reduction for 2 h in an H_2 atmosphere at 550℃, 600℃, or 700℃ at a heating rate of 2 ℃/min to obtain the desired catalyst. The fabricated catalysts were named Ni_3Mo_3N-T, where T is the reduction temperature, for example, Ni_3Mo_3N reduced at 600°C is named Ni_3Mo_3N-600.

1.2.2 Preparation of the Mo_2N catalyst

The specified quantity of molybdenum trioxide was accurately weighed and subjected to heating at a rate of 5 ℃/min under NH_3 atmosphere, reaching a temperature of 700 ℃ for a duration of 2 h. Subsequently, the obtained samples were cooled down to room temperature, resulting in the formation of molybdenum nitride denoted as Mo_2N.

1.2.3 Preparation of the Ni_xN catalyst

The nickel nitrate hexahydrate (5.8 g) and urea (4.9 g) were accurately weighed and dissolved in 50 ml of deionized water at room temperature, followed by stirring for 0.5 h. Subsequently, the resulting mixed solution was transferred to a 100 ml autoclave and maintained at 120 ℃ for 6 h. After cooling the autoclave to room temperature, the solid sample was extracted, filtered, washed with deionized water and ethanol, and then dried at 100 ℃ for 8 h to obtain the catalyst precursor. The dried catalyst precursor was further subjected to heating in an NH_3 atmosphere with a heating rate of 5 ℃/min until reaching a temperature of 380 ℃ for a duration of 3.5 h. Finally, the sample was cooled down to room temperature to yield the nickel nitride catalyst denoted as Ni_xN.

1.3 Catalyst characterization

The structure and crystallinity of the catalysts were analyzed using a Rigaku Ultra IV diffractometer with Cu Kα radiation (γ = 0.152) at a scanning rate of 8° min^{-1}, operating at 40 KV and 10 mA in a 2θ range of 20–80°. The specific surface area (S_{BET}), pore size distribution, and pore volume of the catalyst were determined using an ASAP2020 automatic micropore and chemisorption apparatus. N_2 adsorption–desorption isotherms were measured at −196°C. Scanning electron microscopy (SEM) and energy-dispersive X-ray spectroscopy (EDX) were performed using a Zeiss Sigma 300 scanning electron microscope with an accelerated voltage of 20 kV. Transmission electron microscopy (TEM) images were captured using a JEM-2100 PLUS high-resolution (HR) transmission electron microscope by evenly dispersing the sample in EtOH and placing it on a Cu grid. Raman spectroscopy was performed using a Bruker Senterra instrument with an excitation wavelength of 532 nm. H_2 temperature-programmed desorption (H_2-TPD) and NH_3 temperature-programmed desorption (NH_3-TPD) were performed using XianQuan TP-5080. The metal content of Ni and Mo was measured by the inductively coupled plasma atomic emission spectrometry (ICP-AES). Pyridine adsorption Fourier transform infrared (Py-FT-IR) spectroscopy was performed using a Nicolet iS50 spectrometer. The calculations for the Lewis acid site and Bronsted acid site contents are as follows:

$$C_{(L\ or\ B)} = \frac{K_{L\ or\ B} \times I_{L\ or\ B} \times R^2 \times 1000}{W}$$

The concentration of the Bronsted acid sites or Lewis acid sites is represented by $C_{(L\ or\ B)}$ (unit: μmol g-1), where $K_{L\ or\ B}$ represents the extinction coefficient of the Bronsted acid and Lewis acid, $I_{L\ or\ B}$ represents the peak area of their characteristic peaks, R (unit: cm) denotes the radius of the self-supported molecular sieve tablet, and W (unit: mg) signifies its mass.

1.4 Evaluation of the catalyst performance in the hydrogenation reaction of DMO

The hydrogenation of DMO was performed in a fixed-bed reactor with a length of 300 mm, an inner diameter of 8 mm, and an outer diameter of 16 mm. A stainless-steel fixed-bed reactor with an inner diameter of 8 mm was loaded with 0.28 g of the catalyst. The catalytic performance of the catalyst in the hydrogenation of DMO was evaluated using the continuous flow method. During the reaction, a high-pressure pump was used to introduce the reactant (15 wt.% DMO methanol solution) into the reactor, where it was mixed with hydrogen for the reaction to occur. The catalytic performance of the catalyst was studied at a DMO weight liquid hourly space velocity ($WLHSV_{DMO}$) of 0.1 h^{-1}, a temperature of 280°C, and a pressure of 0.5 MPa. Products were analyzed via gas chromatography (GC) using GC-9790 PLUS (Foley Instrument) equipped with a capillary column (30 m × 0.32 nm × 0.5 μm) and a flame ionization detector (FID).

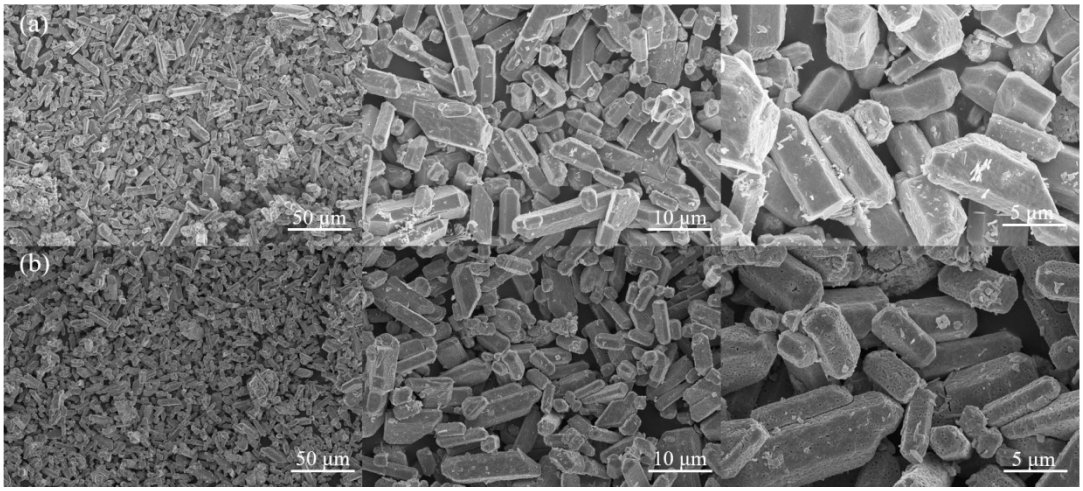

Figure S1. SEM images of (a) Ni_3Mo_3N-550 and (b) Ni_3Mo_3N-700 catalysts

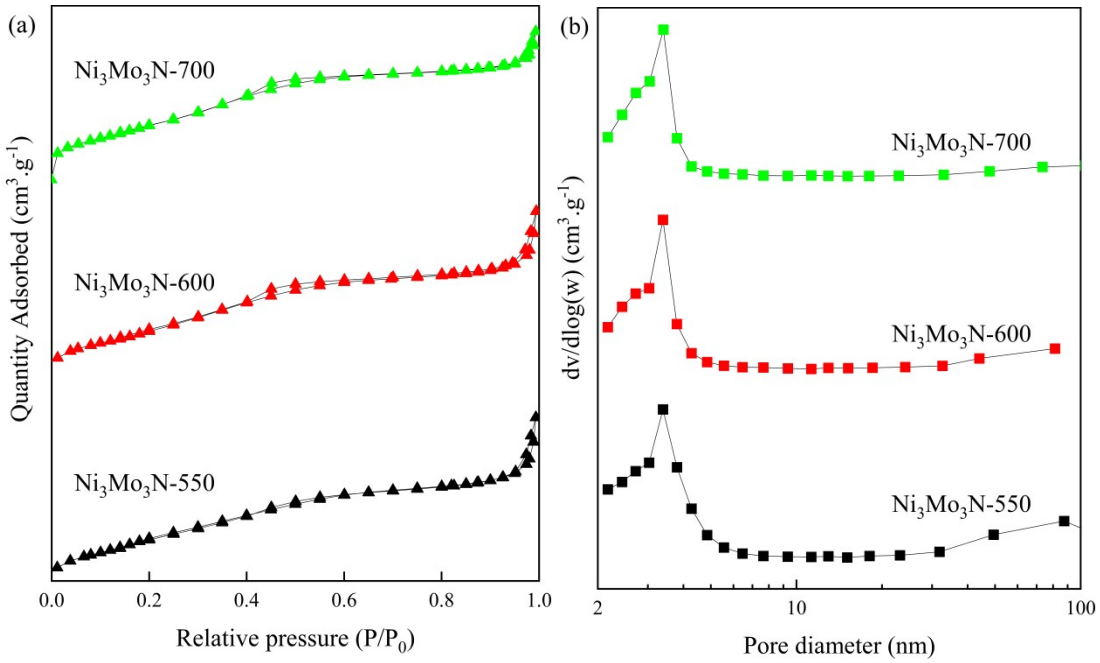

Figure S2. Nitrogen adsorption-desorption isothermal curve (a) and pore size distribution diagram (b) of Ni3Mo3N-T catalysts

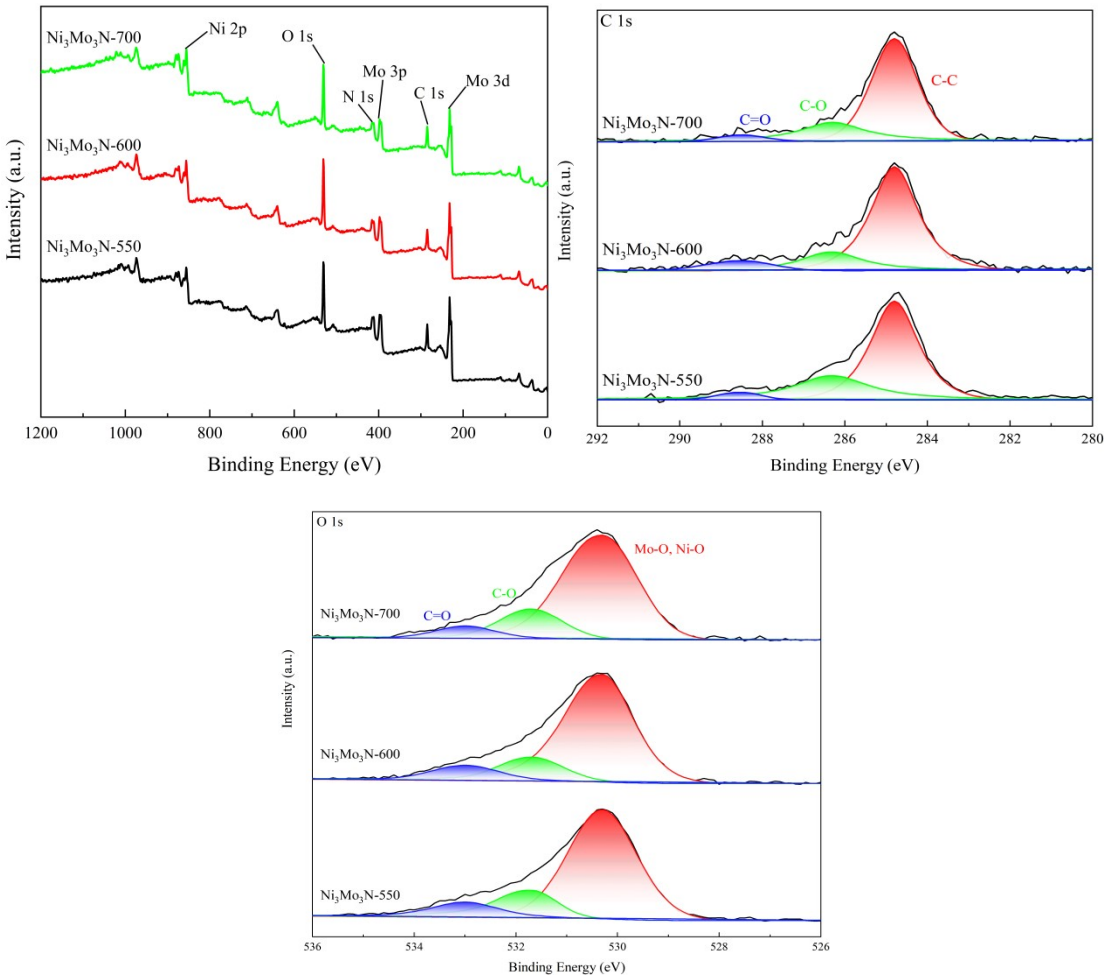

Figure S3. XPS spectra of Survey, C1s, O1s regions of Ni_3Mo_3N-T catalysts

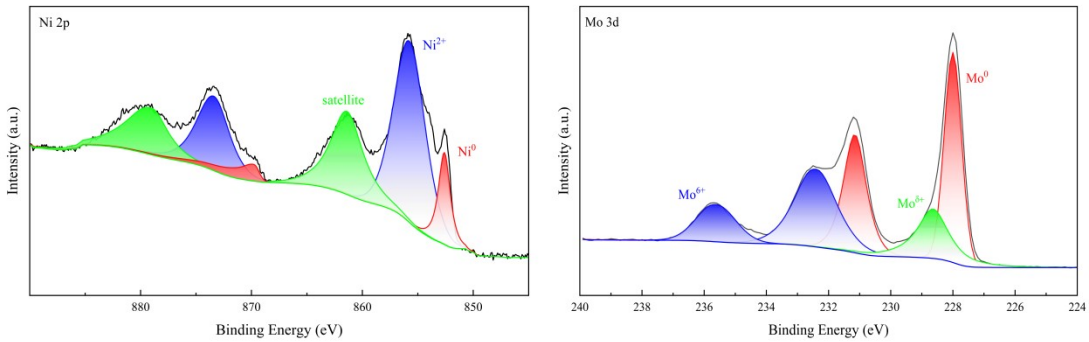

Figure S4. XPS spectra of metal Ni and Mo

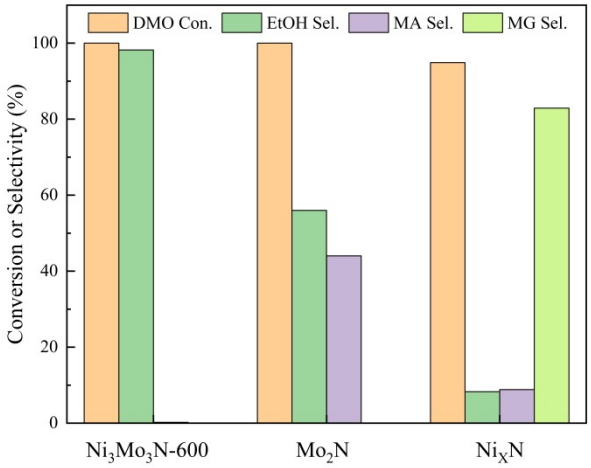

Figure S5. Performance comparison of different catalysts

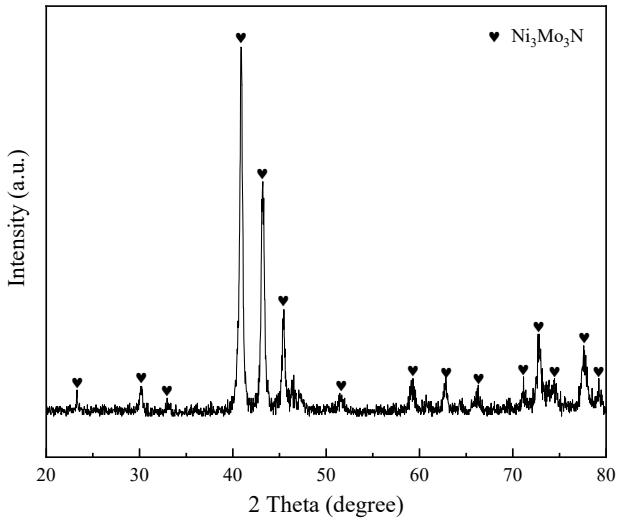

Figure S6. XRD pattern of Ni_3Mo_3N-600 catalyst after reaction

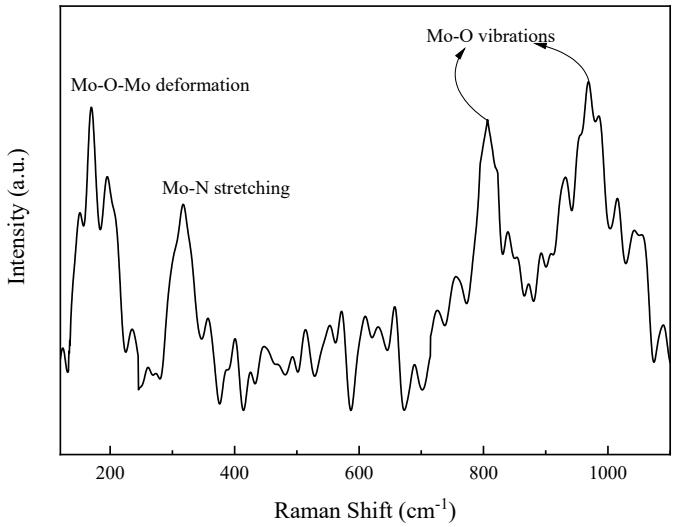

Figure S7. Raman spectra of Ni_3Mo_3N-600 catalyst after reaction

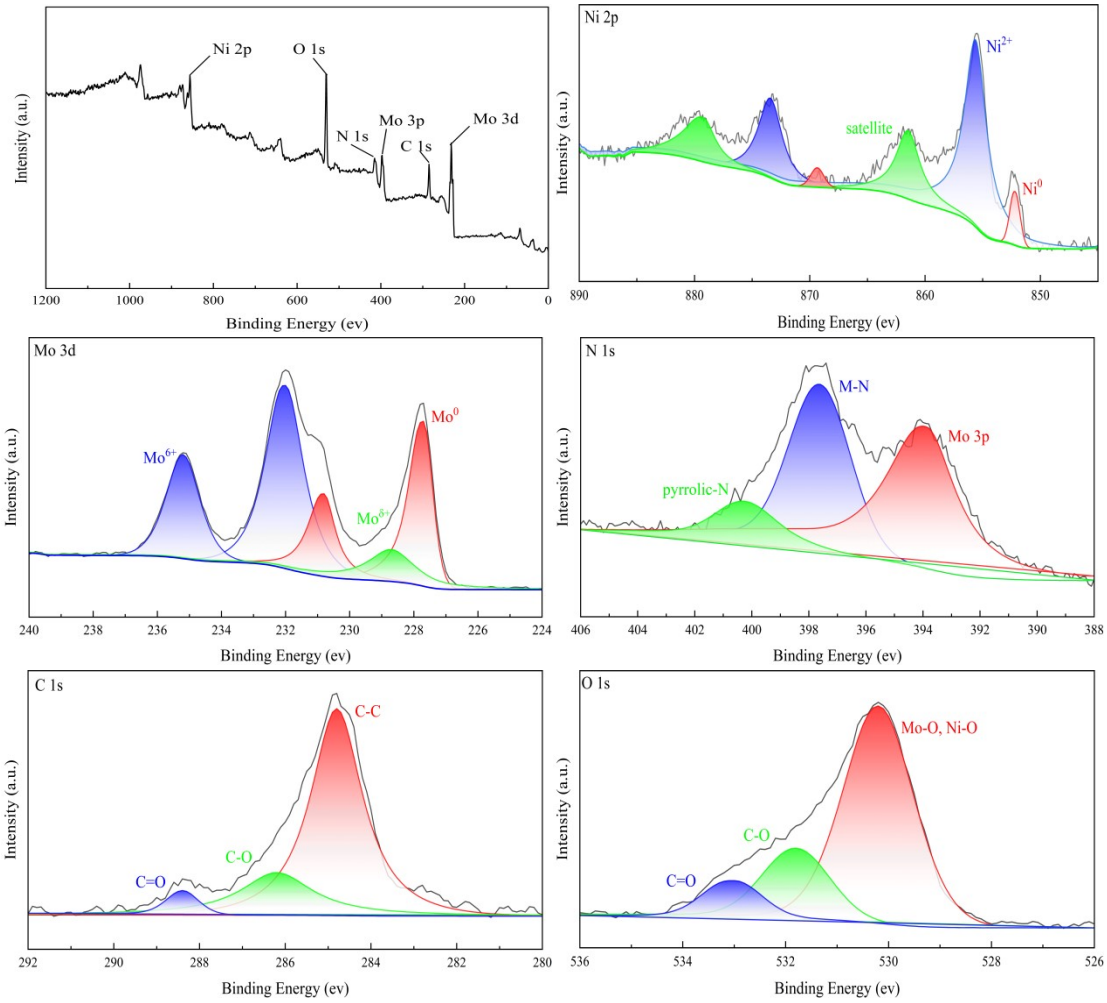

Figure S8. XPS spectra of Ni_3Mo_3N-600 catalyst after reaction

Table S1 The elemental composition of different samples.(from EDX)

Catalysts	Element content (%)				
	Ni	Mo	N	C	O
Ni_3Mo_3N-550	22.52	23.62	8.23	35.41	10.22
Ni_3Mo_3N-600	21.81	22.36	7.41	38.74	9.68
Ni_3Mo_3N-700	21.06	22.21	7.92	39.66	9.15

Table S2 The Elemental mass content in different samples.

Catalysts	Mass content (%)						
	Ni [a]	Mo [a]	Ni [b]	Mo [b]	N [b]	C [b]	O [b]
Ni_3Mo_3N-550	26.84	59.77	27.48	56.42	4.42	8.82	2.86
Ni_3Mo_3N-600	27.46	60.33	28.27	55.68	3.02	9.49	3.54
Ni_3Mo_3N-700	26.09	57.32	26.36	57.33	3.72	10.25	2.34
Ni_3Mo_3N-600 [c]	25.89	59.06					

a Calculated by ICP-AES b Calculated by EDX c after reaction

Table S3 The surface content of different elements obtained from XPS results

Catalysts	Element content (%)				
	Ni	Mo	N	C	O
Ni_3Mo_3N-550	5.46	13.12	28.19	26.38	26.85
Ni_3Mo_3N-600	5.72	12.52	27.42	25.61	28.73
Ni_3Mo_3N-700	5.76	12.21	25.38	29.07	27.58

Table S4 The binding energy and relative content for different species of Ni obtained from XPS.

Catalysts	Ni^0		Ni^{2+}	
	B.E. (eV)	R.C. (%)	B.E. (eV)	R.C. (%)
Ni_3Mo_3N-550	852.3	10.67	855.4	68.39
Ni_3Mo_3N-600	852.2	12.41	855.4	64.65
Ni_3Mo_3N-700	852.2	11.94	855.3	68.54

Table S5 The binding energy and relative content for different species of Mo obtained from XPS.

Catalysts	Mo^0		$Mo^{\delta+}(0 < \delta < 6)$		Mo^{6+}	
	B.E. (eV)	R.C. (%)	B.E. (eV)	R.C. (%)	B.E. (eV)	R.C. (%)
Ni_3Mo_3N-550	227.5	43.71	228.4	12.35	231.8	43.94
Ni_3Mo_3N-600	227.4	41.72	228.4	14.08	231.8	44.20
Ni_3Mo_3N-700	227.5	42.94	228.5	13.17	231.8	43.89

Table S6 Performance of a series of catalysts in DMO hydrogenation to EtOH

Catalyst	T (℃)	P (MPa)	H_2/ DMO(mol)	$WLHSV_{DMO}$ (h^{-1})	DMO Conv. (%)	EtOH Sel.(%)	Life span (h)	Ref
Ni_3Mo_3N	280	**0.5**	**10**	0.1	100	97.5	300	This work
Cu/SiO_2	280	2.5	200	2	100	83	200	[2]
$Cu\text{-}Al/SiO_2$	280	2.5	200	0.2	100	95	40	[3]
$Re\text{-}Cu/SiO_2$	230	1.5	280	0.36	100	90	800	[4]
Mo_3Cu_{20}/SiO_2	280	5.5	450	0.2	100	94	460	[5]
CuMgAl-LDH-1.25	280	3	200	0.5	100	83	100	[6]
Fe_5C_2&CuZnO-SiO_2	260	2.5	180	0.2	100	98	35	[7]
Fe_5C_2	260	2.5	180	0.2	100	89.6	130	[8]
Fe@C	270	4	180	0.19	100	84.3	50	[9]
Fe/ZrO_2	240	2.5	200	0.25	100	94	300	[10]
Fe/mesC-280	260	2.5	180	0.6	100	85.5	100	[11]
$MoNi_4$-MoO_x/Ni-foam	230	2.5	180	0.22	100	93	220	[12]
$25Mo_2C/SiO_2$	200	2.5	200	0.2	100	70.8	350	[13]
$Cu\text{-}Mo_2C$	200	2.5	200	0.2	100	67.2	300	[14]
$FeNi_3$-FeOx/Ni-foam	230	2.5	90	0.44	100	98	700	[15]

References

1. Du, X.; Lei, X.; Zhou, L.; Peng, Y.; Zeng, Y.; Yang, H.; Li, D.; Hu, C.; Garcia, H., Bimetallic Ni and Mo Nitride as an Efficient Catalyst for Hydrodeoxygenation of Palmitic Acid. *ACS Catalysis* **2022,** *12* (8), 4333-4343.
2. Gong, J.; Yue, H.; Zhao, Y.; Zhao, S.; Zhao, L.; Lv, J.; Wang, S.; Ma, X., Synthesis of Ethanol via Syngas on Cu/SiO2 Catalysts with Balanced Cu0–Cu+ Sites. *Journal of the American Chemical Society* **2012,** *134* (34), 13922-13925.
3. Shu, G.; Ma, K.; Tang, S.; Liu, C.; Yue, H.; Liang, B., Highly selective hydrogenation of diesters to ethylene glycol and ethanol on aluminum-promoted CuAl/SiO2 catalysts. *Catalysis Today* **2021,** *368*, 173-180.
4. Du, Z.; Li, Z.; Wang, S.; Chen, X.; Wang, X.; Lin, R.; Zhu, H.; Ding, Y., Stable ethanol synthesis via dimethyl oxalate hydrogenation over the bifunctional rhenium-copper nanostructures: Influence of support. *Journal of Catalysis* **2022,** *407*, 241-252.
5. Li, Z.; Li, Y.; Wang, X.; Tan, Y.; Yang, W.; Zhu, H.; Chen, X.; Lu, W.; Ding, Y., Hydrogenation of dimethyl oxalate to ethanol over Mo-doped Cu/SiO2 catalyst. *Chemical Engineering Journal* **2023,** *454*.
6. Shi, J.; He, Y.; Ma, K.; Tang, S.; Liu, C.; Yue, H.; Liang, B., Cu active sites confined in MgAl layered double hydroxide for hydrogenation of dimethyl oxalate to ethanol. *Catalysis Today* **2021,** *365*, 318-326.
7. Shang, X.; Huang, H.; Han, Q.; Xu, Y.; Zhao, Y.; Wang, S.; Ma, X., Preferential synthesis of ethanol from syngas via dimethyl oxalate hydrogenation over an integrated catalyst. *Chem Commun (Camb)* **2019,** *55* (39), 5555-5558.
8. He, J.; Zhao, Y.; Wang, Y.; Wang, J.; Zheng, J.; Zhang, H.; Zhou, G.; Wang, C.; Wang, S.; Ma, X., A Fe(5)C(2) nanocatalyst for the preferential synthesis of ethanol via dimethyl oxalate hydrogenation. *Chem Commun (Camb)* **2017,** *53* (39), 5376-5379.
9. Sun, Y.; Ma, Q.; Ge, Q.; Sun, J., Tunable Synthesis of Ethanol or Methyl Acetate via Dimethyl Oxalate Hydrogenation on Confined Iron Catalysts. *ACS Catalysis* **2021,** *11* (8), 4908-4919.
10. Abbas, M.; Zhang, J.; Chen, J., Sonochemical engineering of highly efficient and robust Au nanoparticle-wrapped on Fe/ZrO2 nanorods and their controllable product selectivity in dimethyl oxalate hydrogenation. *Catalysis Science & Technology* **2020,** *10* (4), 1125-1134.
11. Cao, M.; Huang, H.; Zheng, Y.; Zhang, Q.; Wang, S.; Ge, R.; Wang, J.; Zhao, Y.; Ma, X., Enhanced Effect of the Mesoporous Carbon on Iron Carbide Catalyst for Hydrogenation of Dimethyl Oxalate to Ethanol. *ChemCatChem* **2022,** *14* (20).
12. Zhu, J.; Sun, W.; Wang, S.; Zhao, G.; Liu, Y.; Lu, Y., A Ni-foam-structured MoNi4–MoOx nanocomposite catalyst for hydrogenation of dimethyl oxalate to ethanol. *Chemical Communications* **2020,** *56* (5), 806-809.
13. Liu, Y.; Ding, J.; Sun, J.; Zhang, J.; Bi, J.; Liu, K.; Kong, F.; Xiao, H.; Sun, Y.; Chen, J., Molybdenum carbide as an efficient catalyst for low-temperature hydrogenation of dimethyl oxalate. *Chem Commun (Camb)* **2016,** *52* (28), 5030-2.
14. Liu, Y.; Ding, J.; Bi, J.; Sun, Y.; Zhang, J.; Liu, K.; Kong, F.; Xiao, H.; Chen, J., Effect of Cu-doping on the structure and performance of molybdenum carbide catalyst for low-temperature hydrogenation of dimethyl oxalate to ethanol. *Applied Catalysis A: General* **2017,** *529*, 143-155.

15. Zhu, J.; Zhao, G.; Sun, W.; Nie, Q.; Wang, S.; Xue, Q.; Liu, Y.; Lu, Y., Superior FeNi3-FeOx/Ni-foam catalyst for gas-phase hydrogenation of dimethyl oxalate to ethanol. *Applied Catalysis B: Environmental* **2020,** *270*.